Hadronic Cross Section Measurements with ISR and the Implications on $g_\mu - 2$

K. Griessinger representing the *BABAR* Collaboration
Mainz University, Institute for Nuclear Physics, J.-J.-Becherweg 45, 55099 Mainz, Germany

The B-Factories have produced data of unprecedented precision for the measurement of hadronic cross sections. This data, extracted via Initial State Radiation (ISR), can be used to predict the anomaly of the muon gyromagnetic factor, $g_\mu - 2$. In this note, the recent *BABAR* -measurements of the channels $e^+e^- \to \pi^+\pi^-\pi^+\pi^-$ and $e^+e^- \to K^+K^-$ are summarized, which improve the accuracy of the Standard Model prediction of $g_\mu - 2$ significantly.

1 Introduction

The muon gyromagnetic factor g_μ can be determined directly from spin precession measurements and theoretically in the Standard Model. For the latter, the QED and weak contributions to $a_\mu \equiv (g_\mu - 2)/2$ can be calculated perturbatively to great precision ($a_\mu^{\mathrm{QED}} = (116\,584\,718.951 \pm 0.080) \cdot 10^{-11}$ [1] and $a_\mu^{\mathrm{weak}} = (154 \pm 2) \cdot 10^{-11}$ [2], respectively). In contrast, the contribution from strong interaction at low energies cannot be calculated perturbatively due to the magnitude of the running strong coupling constant $\alpha_{\mathrm{s}}(s)$. Therefore a dispersion integral (obtained via the optical theorem) is employed to calculate the hadronic low energy part of a_μ from the experimentally determined hadronic cross section $\sigma_{\mathrm{had}}(s)$:

$$a_\mu^{\mathrm{had}}(s \le E_{\mathrm{cut}}^2) = \frac{1}{4\pi^3} \int_{m_\pi^2}^{E_{\mathrm{cut}}^2} K(s)\sigma_{\mathrm{had}}(s)\mathrm{d}s \ .$$

$K(s)$ denotes the analytically known [3] Kernel function, which exhibits an asymptotic $1/s$ decrease. The value of E_{cut} is chosen such that $\alpha_{\mathrm{s}}(s)$ is sufficiently small for $s > E_{\mathrm{cut}}^2$ and thus the remaining part $a_\mu^{\mathrm{had}}(s > E_{\mathrm{cut}}^2)$ can be calculated in a perturbative expansion. This combination leads to a value of approximately $a_\mu^{\mathrm{had}} = (6930 \pm 49) \cdot 10^{-11}$ [2].

On the purely experimental side, a_μ is determined by measuring the difference of the Larmor and Cyclotron frequency of precessing muons. This led to a very precise measurement in the E821 experiment at Brookhaven National Laboratory with the result $a_\mu = (116\,592\,089 \pm 54_{\mathrm{stat}} \pm 33_{\mathrm{syst}}) \cdot 10^{-11}$ [2].

The direct and theoretical results deviate by approximately 3.5σ. Since this discrepancy merely provides a hint at yet no evidence for a deficiency in the Standard Model, more precise data from both sides is of utmost importance.

2 Experimental Setup

The B-Factories *BABAR* and Belle are located at SLAC National Accelerator Center in Stanford, USA and at KEK in Tsukuba, Japan, respectively. *BABAR* achieved an integrated luminosity of $\sim 530\,\mathrm{fb}^{-1}$, whereas Belle even exceeded $1\,\mathrm{ab}^{-1}$. While running (mostly) at the $\Upsilon(4S)$ resonance, this produced a large data set for the study of hadronic cross sections via the process of Initial State Radiation (ISR). This process takes place when one of the particles in the initial state (e^+e^-) radiates a photon. Since the photon carries a certain amount of CMS-energy E_γ^*, the squared center-of-mass energy s ist lowered to $s' = s - 2\sqrt{s}E_\gamma^*$. Owed to the continuous spectrum of possible photon energies, this gives access to a broad range of invariant masses over which hadronic cross sections may be measured.

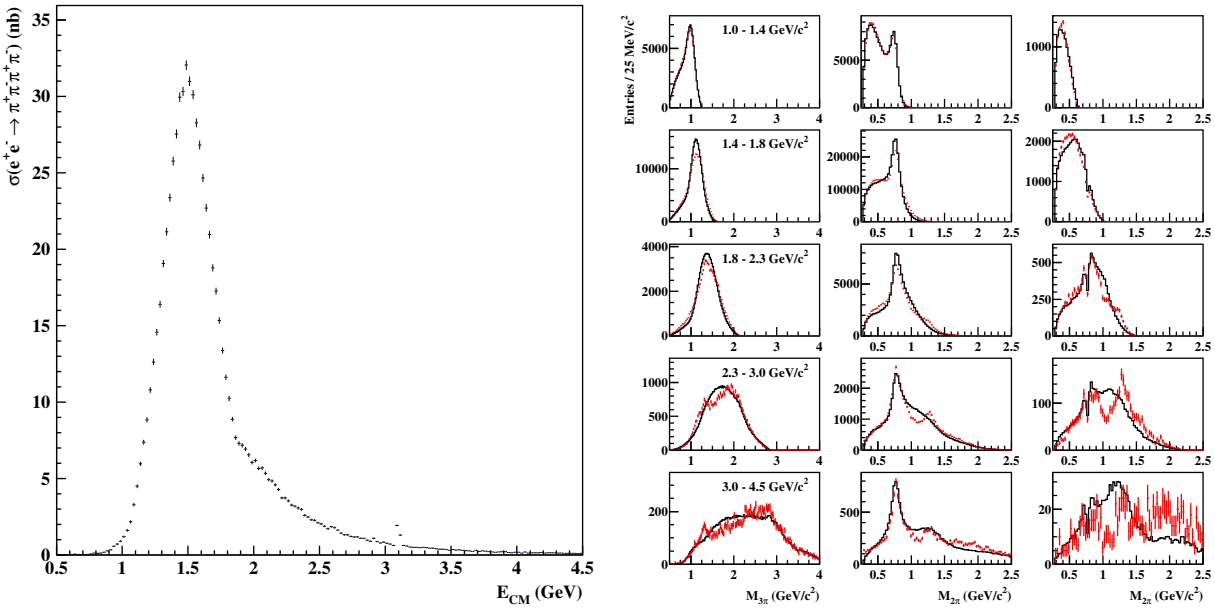

Figure 1: Left panel: The cross section $e^+e^- \to \pi^+\pi^-\pi^+\pi^-$ measured at *BABAR* . Statistical uncertainties only, systematics are listed in Tab. 1. Right panel: Internal structures, data in red, simulation in black. From top to bottom: slices in the 4π invariant mass. Left to right: 3π mass, 2π mass and 2π not originating from ρ^0.

3 Measurement of the channel $e^+e^- \to \pi^+\pi^-\pi^+\pi^-$ [4]

The channel $e^+e^- \to \pi^+\pi^-\pi^+\pi^-$ is not only interesting for its cross section, but also due to its rich internal structures. These are explored by investigating the invariant masses of different particle combinations from the final state as a function of the total invariant mass of the hadronic system, see Fig. 1 (right). In the three-pion mass (left column, 4 entries per event for all combinations), the $a_1(1260)$ is observed clearly, especially in the high-mass slices. The charge neutral two-pion mass, which also contains 4 combinations per event, exhibits a very pronounced ρ^0 signature. This peak contains approximately one fourth of all entries in each histogram. Since $e^+e^- \to \rho^0\rho^0$ is forbidden at tree level, this means that there must be one ρ^0 in each event. When excluding the $\pi^+\pi^-$ combination from the ρ^0, the third column of Fig. 1 (right) is produced. Here, the additional resonances apart from the ρ^0 show up much more clearly. In the spectrum, especially the $f_0(980)$ and $f_2(1270)$ can be observed quite nicely at intermediate and large total hadronic energies.

The cross section itself is shown in Fig. 1 (left) with its statistical uncertainties. The systematics are listed in Tab. 1. This very precise measurement improves the low-energy ($0.6\,\text{GeV} < \sqrt{s} < 1.8\,\text{GeV}$) prediction of $a_\mu^{\text{had}}(\pi^+\pi^-\pi^+\pi^-)$ from $a_\mu^{\text{had}}(\pi^+\pi^-\pi^+\pi^-) = (133.5 \pm 1.0_{\text{stat}} \pm 5.2_{\text{syst}}) \cdot 10^{-11}$, calculated using the previous world data set (including the smaller *BABAR* data set from 2006), to $a_\mu^{\text{had}}(\pi^+\pi^-\pi^+\pi^-) = (136.4 \pm 0.3_{\text{stat}} \pm 3.6_{\text{syst}}) \cdot 10^{-11}$, only with the *BABAR* measurement.

Table 1: Systematic uncertainties of the $e^+e^- \to \pi^+\pi^-\pi^+\pi^-$ cross section measured at *BABAR* .

M_{had}	$< 1.1\,\text{GeV}$	$1.1\,\text{GeV} \leq M_{\text{had}} \leq 2.8\,\text{GeV}$	$> 2.8\,\text{GeV}$
σ_{syst}	11 %	2.4 %	4 %

4 Measurement of the channel $e^+e^- \to K^+K^-$ [5]

Another channel that had yet to be measured with high precision was the production of two charged Kaons. At *BABAR* it has now been analyzed using $\sim 232\,\text{fb}^{-1}$, yielding the cross section with a very large ϕ peak shown in Fig. 2. Remarkably small uncertainties down to 0.7 % in

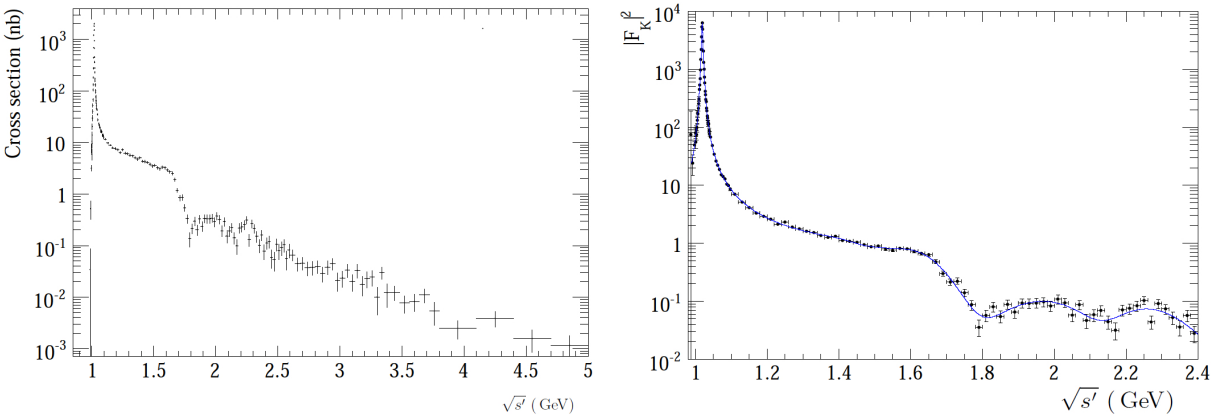

Figure 2: Cross section $e^+e^- \to K^+K^-$ measured at *BABAR* (left, J/ψ and $\psi(2S)$ removed) and the corresponding squared Kaon form factor (right) including a BW-fit (blue). Statistical and systematic uncertainties shown.

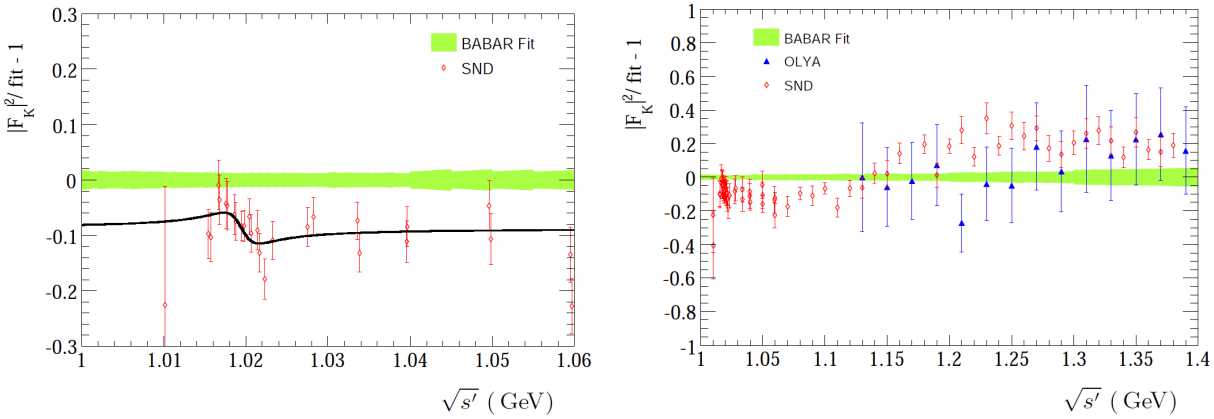

Figure 3: Deviation between the fit to the squared Kaon form factor measured at *BABAR* and SND data in the ϕ region (left) and in a wider energy range (right), also including OLYA.

the ϕ peak region were achieved especially by very diligently studying Kaon particle (mis-)-identification and the ISR-luminosity, which is calculated from $e^+e^- \to \mu^+\mu^-\gamma$ event rates.

From this cross section, the corresponding form factor is extracted, see Fig. 2. It is parametrized by a sum of Breit-Wigner distributions:

$$\begin{aligned} F_K(s) &= (a_\phi \cdot BW_\phi(s) + a_{\phi'} \cdot BW_{\phi'}(s) + a_{\phi''} \cdot BW_{\phi''}(s))/3 \\ &+ (a_\rho \cdot BW_\rho(s) + a_{\rho'} \cdot BW_{\rho'}(s) + a_{\rho''} \cdot BW_{\rho''}(s) + a_{\rho'''} \cdot BW_{\rho'''}(s))/2 \\ &+ (a_\omega \cdot BW_\omega(s) + a_{\omega'} \cdot BW_{\omega'}(s) + a_{\omega''} \cdot BW_{\omega''}(s) + a_{\omega'''} \cdot BW_{\omega'''}(s))/6 \\ \text{with} \quad & a_\phi + a_{\phi'} + a_{\phi''} = 1 \ , \ a_\rho + a_{\rho'} + a_{\rho''} + a_{\rho'''} = 1 \ , \ a_\omega + a_{\omega'} + a_{\omega''} + a_{\omega'''} = 1 \ . \end{aligned}$$

Using the fit to the *BABAR* data, the results from other experiments can be compared to *BABAR* . This is shown in Fig. 3 and some interesting deviations are found. There is a small wiggle around the ϕ mass, which is due to calibration differences of the experiments and is covered by the experimental uncertainties. More importantly for the determination of $g_\mu - 2$, there seems to be a normalization difference between data from *BABAR* and the experiments from Novosibirsk (SND and CMD2). While in the low-mass region around the ϕ SND and CMD2 show a smaller form factor, above $\sqrt{s'} \approx 1.15\,\text{GeV}$ the form factor from SND is considerably larger (CMD2 has not yet published their result in the full energy range).

Furthermore the measurement of the form factor can be compared to theoretical predictions [6,7] in the high-energy regime. For large values of $\sqrt{s'}$,

$$\|F_K(s')\|^2 = 64\pi^2 f_K^4 \cdot \frac{\alpha_s^2(s')}{s'^n}$$

with $n = 2$ is predicted in a perturbative approach. While the measurement confirms the exponent with a fitted (in the regime $\sqrt{s'} > 2.5\,\text{GeV}$) value of $n = 2.10 \pm 0.23$ and agrees with the point from CLEO at $\sqrt{s'} \approx 3.8\,\text{GeV}$, the overall scaling is off by roughly a factor of 20, as seen in Fig. 4. This effect has yet to be understood.

For the SM prediction of $g_\mu - 2$, this new cross section measurement dramatically improves the precision in the energy range $0.98\,\text{GeV} < \sqrt{s} < 1.8\,\text{GeV}$ from $a_\mu^{\text{had}}(K^+K^-) = (216.3 \pm 2.7 \pm 6.8) \cdot 10^{-11}$ with the previous world data set to $a_\mu^{\text{had}}(K^+K^-) = (229.5 \pm 1.4 \pm 2.2) \cdot 10^{-11}$ only on *BABAR* data.

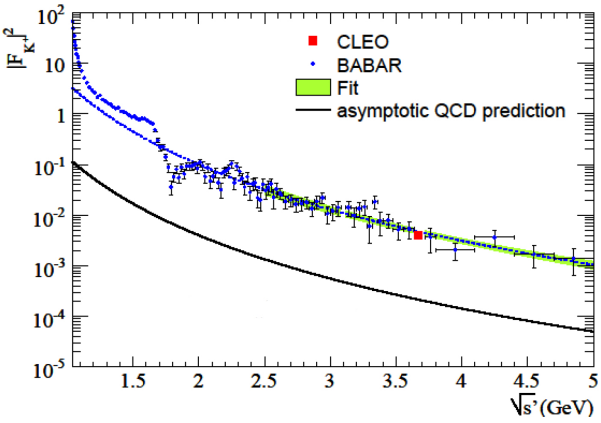

Figure 4: Comparison of the squared Kaon form factors between data and theory the from asymptotic QCD.

5 Conclusions

The recent *BABAR* results on the $e^+e^- \to \pi^+\pi^-\pi^+\pi^-$ and $e^+e^- \to K^+K^-$ cross sections reach unprecedented accuracy. Consequently, they have significantly improved the precision of the SM prediction for $g_\mu - 2$. Furthermore interesting intermediate structures were found in the 4π channel and the Kaon form factor stands in stark contrast to the high-energy QCD prediction.

Acknowledgments

We would like to thank the organizers for a great conference. We are grateful for the excellent luminosity and machine conditions provided by our PEP-II colleagues, and for the substantial dedicated effort from the computing organizations that support *BABAR* . The collaborating institutions wish to thank SLAC for its support and kind hospitality. This work is supported by DOE and NSF (USA), NSERC (Canada), CEA and CNRS-IN2P3 (France), BMBF and DFG (Germany), INFN (Italy), FOM (The Netherlands), NFR (Norway), MES (Russia), MICIIN (Spain), STFC (United Kingdom). Individuals have received support from the DFG (Germany).

References

1. Tatsumi Aoyama, Masashi Hayakawa, Toichiro Kinoshita, and Makiko Nio. Complete Tenth-Order QED Contribution to the Muon $g-2$. *Phys.Rev.Lett.*, 109:111808, 2012.
2. Michel Davier, Andreas Hoecker, Bogdan Malaescu, and Zhiqing Zhang. Reevaluation of the Hadronic Contributions to the Muon $g-2$ and to $\alpha(M_Z)$. *Eur.Phys.J.*, C71:1515, 2011.
3. N.N. Achasov and A.V. Kiselev. Contribution to muon $g-2$ from the $\pi^0\gamma$ and $\eta\gamma$ intermediate states in the vacuum polarization. *Phys.Rev.*, D65:097302, 2002.
4. J.P. Lees et al. Initial-State Radiation Measurement of the $e^+e^- \to \pi^+\pi^-\pi^+\pi^-$ Cross Section. *Phys.Rev.*, D85:112009, 2012.
5. Michel Davier. e^+e^- results from BABAR and implications for $g-2$. 2013. arXiv:1302.1907.
6. V.L. Chernyak, A.R. Zhitnitsky, and V.G. Serbo. Asymptotic hadronic form-factors in quantum chromodynamics. *JETP Lett.*, 26:594–597, 1977.
7. G. Peter Lepage and Stanley J. Brodsky. Exclusive Processes in Quantum Chromodynamics: Evolution Equations for Hadronic Wave Functions and the Form-Factors of Mesons. *Phys.Lett.*, B87:359–365, 1979.